Electron transfer and localization in endohedral metallofullerenes: *Ab initio* density functional theory calculations

Shenyuan Yang,[1,2,3] Mina Yoon,[3,2] Christian Hicke,[4] Zhenyu Zhang,[3,2] and Enge Wang[1]
[1]*International Center for Quantum Structures and Institute of Physics, Chinese Academy of Sciences, Beijing 100190, People's Republic of China*
[2]*Department of Physics and Astronomy, The University of Tennessee, Knoxville, Tennessee 37996, USA*
[3]*Materials Science and Technology Division, Oak Ridge National Laboratory, Oak Ridge, Tennessee 37831, USA*
[4]*Department of Physics and Astronomy, Michigan State University, East Lansing, Michigan 48823, USA*
(Received 15 April 2008; revised manuscript received 16 June 2008; published 26 September 2008)

Endohedral metallofullerenes constitute an appealing class of nanoscale building blocks for fabrication of a wide range of materials. One open question of fundamental importance is the precise nature of charge redistribution within the carbon cages (C_n) upon metal encapsulation. Using *ab initio* density functional theory, we systematically study the electronic structure of metallofullerenes, focusing on the spatial charge redistribution. For large metallofullerenes ($n>32$), the valence electrons of the metal atoms are all transferred to the fullerene states. Surprisingly, the transferred charge is found to be highly localized inside the cage near the metal cations rather than uniformly distributed on the surfaces of the carbon cage as traditionally believed. This counterintuitive charge localization picture is attributed to the strong metal-cage interactions within the systems. These findings may prove to be instrumental in the design of fullerene-based functional nanomaterials.

DOI: 10.1103/PhysRevB.78.115435 PACS number(s): 81.05.Tp, 61.48.−c, 73.22.−f

I. INTRODUCTION

The electronic properties of endohederal metallofullerenes have been intensively explored[1,2] since their initial discovery,[3] with a wide range of potential applications envisioned.[4] In a metallofullerene, the valence electrons are transferred from one or several metal atoms to their enclosing carbon fullerene cage due to the higher electron affinity of the cage.[5–8] The transferred electrons are generally assumed to be delocalized over the covalently bonded carbon cage due to the delocalization nature of the carbon π orbitals.[9] This charge delocalization picture seems to be supported by experimental[10] and theoretical studies.[11] Even in studies showing strong metal-fullerene hybridization,[12–17] the transferred charge is considered to be primarily delocalized over the cage. Thus, metallofullerenes have been regarded as "superatoms"[2] or stable ion pairs[18] that consist of a positively charged metal core surrounded by a homogeneously negatively charged carbon cage. The formal charge state of lanthanum metallofullerenes, for example, is expressed as $La^{3+}@C_{82}^{3-}$. Based on such an electron delocalization picture, partially filled bands in metallofullerene solids has been considered to give rise to conducting or superconducting materials,[19] similar to the case of alkali-intercalated fullerides. In spite of the fundamental importance of understanding the spatial charge distribution in metallofullerenes, most studies have focused on the amount of charge transfer in describing their electronic properties, with little effort devoted to the actual spatial distribution of the transferred charge.[14] To date, the charge delocalization picture based on rather intuitive assumptions has been widely accepted even though its definitive proof is still lacking.

In this paper, we use *ab initio* density functional theory (DFT) to systematically study the electronic structure of metallofullerenes. In order to understand the spatial charge distribution of a metallofullerene as a function of the fullerene size and the type of metal atoms, we start by considering a single La atom encapsulated by different fullerenes such as ($La@C_n$) with $n=28(T_d)$, $32(C_2)$, $50(D_{5h})$, $60(I_h)$, $74(D_{3h})$, $76(T_d)$, and $82(C_{2v})$. Then, we extend the study to different metal atoms (M) inside a C_{82} cage ($M@C_{82}$, where $M=$Li, Ca, Sc). We find that for large metallofullerenes ($n>32$) all the valence electrons of the metal atom are indeed transferred to the fullerene states, yet they are highly localized inside the fullerene and near the metal atom regardless of the type of metal or fullerene. This charge localization picture is due to the strong electrostatic attraction within the cage and is contrary to the generally accepted view. The picture established in the present study has to be adopted when determining important physical properties of metallofullerenes, such as their dipole moments, which sensitively depend on the precise spatial charge distribution within the systems. The rest of the paper is organized as follows. In Sec. II, we present our calculation methods and considered structures. In Sec. III we present the calculation results and discuss in detail the charge localization behavior of the transferred charge in metallofullerenes. Finally, a short summary will be given in Sec. IV.

II. THEORETICAL MODELING

We performed *ab initio* DFT to systematically study the electronic properties of metallofullerenes. We considered different kinds of metallofullerenes such as fullerenes containing a single La atom ($La@C_n$) with $n=28(T_d)$, $32(C_2)$, $50(D_{5h})$, $60(I_h)$, $74(D_{3h})$, $76(T_d)$, and $82(C_{2v})$. Also, C_{82} cages containing different metal atoms (M) inside ($M@C_{82}$, where $M=$Li, Ca, Sc) were studied. Structure optimization and electronic structure calculations were performed using the VIENNA AB INITIO SIMULATION PACKAGE (VASP),[20] with the exchange-correlation potential described by the Ceperley-Alder local-density approximation (LDA).[21] We

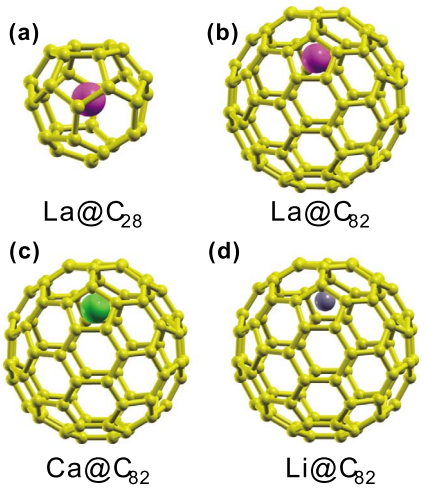

FIG. 1. (Color online) Structures of (a) La@C_{28}, (b) La@C_{82}, (c) Ca@C_{82}, and (d) Li@C_{82}. The C, La, Ca, and Li atoms are denoted by yellow (small light gray), purple (big dark gray), green (big light gray), and gray (medium gray) balls, respectively.

employed the projector-augmented wave pseudopotentials[22] to describe the interaction between ion cores and valence electrons. The energy cutoff for the plane-wave basis set was 400 eV and only Γ point was used for *k*-point sampling.[23] We chose a $22\times22\times22$ Å^3 supercell, allowing a vacuum of at least 14.5 Å between fullerenes of neighboring images. All the structures were fully relaxed until the force on each atom was less than 0.01 eV/Å. Some of studied structures are displayed in Fig. 1.

We have tested the LDA results by comparing with those from generalized gradient approximation (GGA),[24] and reached the same qualitative conclusions. Furthermore, we compared our results using a different calculation method. For selective systems we study their charge redistribution using the SIESTA code.[25] We use Troullier-Martins[26] norm-conserving pseudopotentials with LDA approximation[21] and the basis of split valence double-ξ plus polarization orbitals (DZP).[27] The charge density and potential were calculated on a real-space grid with cut-off energy of 200 Ry. Mulliken population analysis[28] was performed to analyze the bonding properties. We found that the structural and electronic properties obtained from these two calculation methods are qualitatively similar to each other although minor quantitative differences are present. In the following, we will mainly present the results from VASP with LDA approximation, unless otherwise specified.

III. RESULTS AND DISCUSSIONS

Different metal atoms have been successfully encapsulated in fullerenes experimentally, including group III elements such as La and Y[5–8] and group II elements such as Ca.[6] Our calculations show that the La atom is located at the center of the fullerene if $n\leq32$, while it is off centered inside larger fullerenes ($n\geq50$). This observation is consistent with mass spectra measurements showing that the smallest possible La endohedrally doped fullerenes consist of $n=36$ carbon atoms.[29] For La@C_{28}, the distance between La and C atom is ~2.45 Å, which is close to the sum of the covalent radii of these two elements [Fig. 1(a)] while the metal atom of Li, Ca, or La in C_{82} is significantly off centered toward the hexagonal ring along the C_2 axis [Figs. 1(b)–1(d)]. The distance between the La and the nearest C atom of C_{82} is 2.51 Å, in good agreement with previous studies.[7,8,13]

In Fig. 2 we present the partial density of states (PDOS) of different metallofullerenes and their respective pristine fullerenes. Upon metal encapsulation, the carbon levels shift downward and some of these levels become occupied, indicating a net charge transfer from the metal atom to the carbon cage. For small metallofullerenes ($n=28$ and 32), the La atom forms chemical bonds with some carbon atoms and the strong La-C hybridization hinders a complete charge transfer of the three La valence electrons to the carbon cage. As a result, the remaining valence electrons of the La atom occupy states below the Fermi level (E_F) [see Fig. 2(b)]. On the other hand, for large metallofullerenes ($n\geq50$), there is a negligible amount of La valence states (6*s* and 5*d*) below E_F. Three additional fullerene π states are occupied upon La encapsulation, as seen by comparing Figs. 2(c) and 2(d).

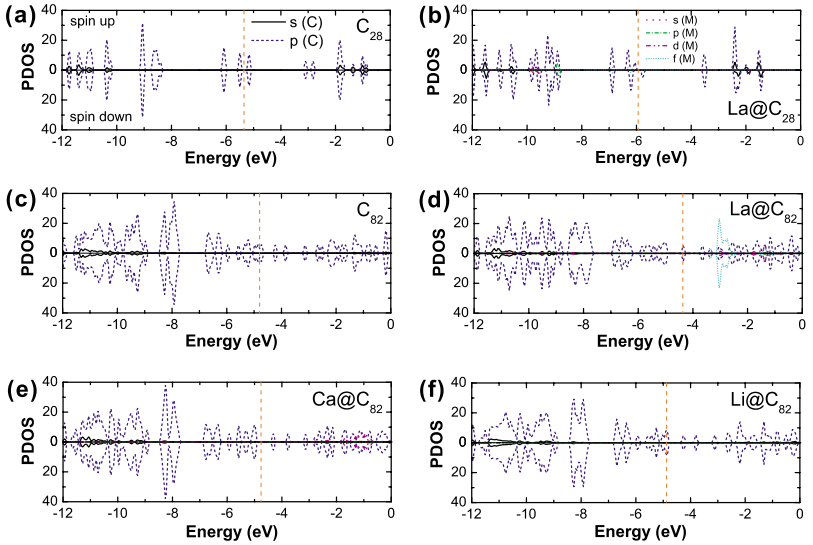

FIG. 2. (Color online) PDOSs of (a) C_{28}, (b) La@C_{28}, (c) C_{82}, (d) La@C_{82}, (e) Ca@C_{82}, and (f) Li@C_{82}. The Fermi level (E_F) is set as energy zero and denoted by vertical dashed line for each panel. The carbon *s* and *p* components are represented by black solid and blue (dark gray) dash lines, respectively, while the metal *s*, *p*, *d*, and *f* components are represented by red (dark gray) dot, green (gray) dash-dot, purple (dark gray) dash-dot-dot, and cyan (gray) short-dot lines, respectively.

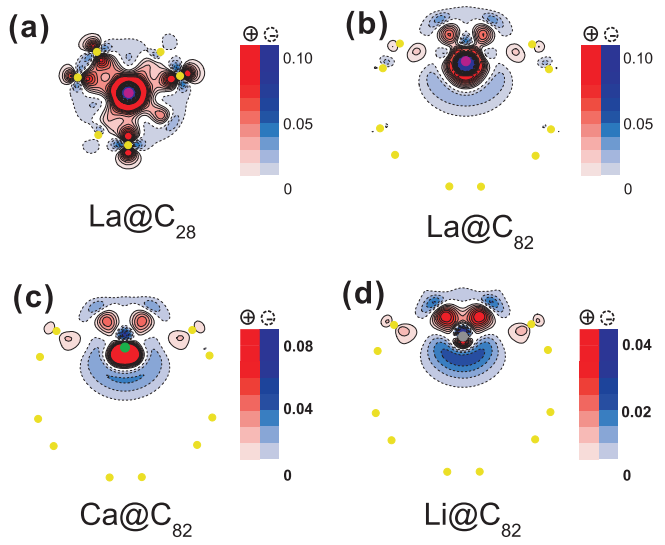

FIG. 3. (Color) Difference electron densities ($\Delta\rho$, in unit of $e/Å^3$) of (a) $La@C_{28}$, (b) $La@C_{82}$, (c) $Ca@C_{82}$, and (d) $Li@C_{82}$. Red (in between solid lines) represents the region of charge accumulation ($\Delta\rho>0$) and blue (in between dotted lines) the region of charge depletion ($\Delta\rho<0$). The plane goes through the centroid of the fullerene cage and the metal atom.

Therefore, we conclude that the La atom has transferred its three valence electrons to the carbon cage if $n\geq 50$. This conclusion is in agreement with experimental measurements where three-electron transfer from La to the carbon cage has been confirmed.[5–7] Similar analysis has been applied to the other types of metallofullerenes. For example, the nondegenerate C_{82} lowest unoccupied molecular orbitals (LUMO) becomes doubly and singly occupied for $Ca@C_{82}$ [Fig. 2(e)] and $Li@C_{82}$ [Fig. 2(f)], respectively, corresponding to transfer of two or one valence electrons to C_{82} from Ca or Li.

As a comparison, we also performed the Mulliken charge analysis of the amount of the localized charge on the La atoms. We found that the Mulliken analysis systematically underestimates the amount of the transferred charge. For example, the La atom inside C_{82} transfers only 1.59 electrons to the fullerene cage. The Mulliken analysis is informative only if we compare the relative charges between the obtained values. For example, it correctly demonstrates that the amount of transferred charges in small metallofullerenes ($n\leq 32$) is smaller than that in large metallofullerenes ($n\geq 50$). In fact, the inaccuracy of the Mulliken analysis has been reported in the literature.[14,15,30] The PDOS analysis, on the other hand, yields more accurate values of the transferred charge, which is consistent with both experiments and previous calculations.

Next, we analyze the spatial distribution of the transferred electrons. The difference charge density $\Delta\rho$ is defined as $\Delta\rho=\rho(M@C_n)-\rho(C_n)-\rho(M)$, where $\rho(M@C_n)$ is the charge density of the metallofullerene, $\rho(C_n)$ is the charge density of the isolated C_n, and $\rho(M)$ is the charge density of the metal (M) atom. As shown in Fig. 3, the transferred electrons are accumulated in a highly localized fashion: excess electrons are mostly distributed near the metal inside the cages and the electron depletion around the metal atom indicates a loss of its valence electrons. No noticeable electron gain is obtained on the fullerenes and all the transferred electrons are effectively screened by the cages, whereas some C atoms even lose their σ electrons. We found that all the large metallofullerenes considered ($n>32$) share essentially the same features regardless of the type of metal or fullerene. However, for small metallofullerenes such as $La@C_{28}$, the inner spaces of the fullerene cages are too narrow to accommodate all the transferred electrons, part of which are spreading onto the cage, filling some carbon π orbitals [Fig. 3(a)]. The charge localization picture is further confirmed by plotting $\Delta\rho$ calculated using SIESTA although the detailed charge redistribution exhibits some minor quantitative differences. For example, the electron density calculated using the localized basis set shows spatially more localized excess electrons than that from the plane-wave basis set.

At first glance, this observation seems to be inconsistent with the PDOS analysis shown in Fig. 2, demonstrating the transfer of all-valence electrons from the metal to the fullerene π orbitals. This seemingly contradictory behavior can be ascribed to the strong ionic interactions between the metal and the fullerene, which strongly modify the spatial distribution of the fullerene-derived states. By analyzing each orbital before and after metal encapsulation, we find that the shapes of the C_{82} π orbitals near the hexagonal ring along the C_2 axis are strongly distorted upon metal encapsulation. These orbitals develop a long tail inside the cage toward the metal atom and slightly shrink outside the cage, while the π orbitals far away from the La atom are scarcely influenced. As a result, the total electron density near the metal atom, and between metal and its neighboring C atoms is enhanced while electron depletion outside the cage and near the hexagonal ring is observed, as shown in Figs. 3(b)–3(d).

Our findings clearly demonstrate that the currently accepted view of a metallofullerene, where the carbon cage is

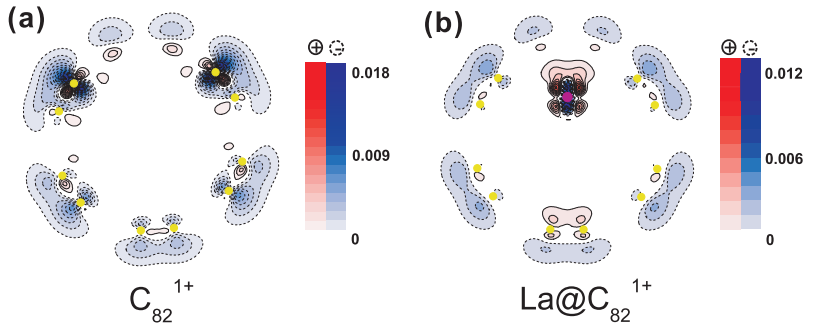

FIG. 4. (Color) (a) The distribution of the extra hole (in unit of $e/Å^3$) in C_{82}^{1+} ion. (b) The distribution of the extra hole in $(La@C_{82})^{1+}$ ion. Red (in between solid lines) represents the region of charge accumulation ($\Delta\rho>0$) and blue (in between dotted lines) the region of charge depletion ($\Delta\rho<0$).

treated as a fullerene ion, needs to be corrected. In particular, the strong metal-fullerene interaction has not been properly accounted for in the prevailing view. For a given metallofullerene, the metal ion attracts the electrons according to electrostatic interactions, which in turn overcome the energy cost associated with the electron localization inside the cage. This explanation is further supported by our calculations showing that the transferred charge enhances the C_{82} π orbitals over the whole cage if the La atom is fixed at the center of the cage. In this case, weak metal-fullerene interion interactions cannot overcome the energy cost due to electron localization. For this highly constrained geometry whose energy is 5.71 eV higher than that of the optimized structure, one La-derived state is occupied just below E_F, indicating that there are only two electrons transferred to C_{82}.

The metal-fullerene interactions have been characterized in terms of electrostatic,[7,8] ionic,[31,32] covalent,[14,31,33] or due to polarization effects.[34] The charge accumulation between the metal atom and fullerene might be regarded as indicative of covalent bond formation. However, detailed Mulliken population analysis shows that the M-C orbital overlaps range between $\sim$0.01 electrons and $\sim$0.08 electrons, much smaller than those of covalently bonded C atoms ($\sim$0.5 electrons) (by one order of magnitude). We therefore conclude that the M-C interactions are largely ionic rather than covalent. The localization of the transferred electrons is a general feature that originated from the electrostatic interaction within the metallofullerenes. This electrostatic interaction distorts and polarizes the fullerene π orbitals close to the metal atom, thus electron accumulates inside the cage.

Various important physical properties, such as the electric-dipole moments and dipolar fields, depend sensitively on the spatial charge distribution, and incorrect assumptions on the charge distribution would result in wrong conclusions. Taking $La@C_{82}$ as an example, if three La valence electrons were delocalized on the C_{82} cage and the off-center distance of the La atom from the centroid of the cage is 1.96 Å, we would obtain a molecular dipole moment of $\sim$28.8 debye. However, a fully relaxed electron-ion distribution calculation shows that the value is only 2.2 debye, one order of magnitude smaller than the above prediction; i.e., the resulting dipolar field of $La@C_{82}$ is negligibly small despite the huge intramolecular charge transfer. We note that previous theoretical calculations obtained similar values of 3–4 debye or smaller,[11,15,30] and some of these studies even discussed the strong hybridization between metal and carbon orbitals. Both of the two observations imply that the charge delocalization picture is not valid, but none of these studies explicitly addressed the issue of precise spatial charge redistribution.

Finally, we comment on metallofullerene ions with net charges produced by metal ion implantation techniques.[35] For pristine fullerenes, an imposed extra charge is evenly distributed over the cage. In the case of charged metallofullerenes, we find that the additional charge is also primarily delocalized over the carbon cage. For example, Figs. 4(a) and 4(b) display the hole distribution of a fullerene ion $(C_{82})^{1+}$ and a metallofullerene ion $(La@C_{82})^{1+}$, respectively, both showing similar charge delocalization behaviors. Here we should emphasize that only the extra charge is delocalized over the cage while the transferred charge from the encaged metal atom is still localized inside the cage. The delocalization of the extra charge in metallofullerene ions might be misleading, and our calculations clarify the distinction between the extra charge and transferred charge.

IV. SUMMARY

To summarize, we have investigated systematically the electronic structure of metallofullerenes, focusing on the spatial charge redistribution. We found that for large metallofullerenes ($n > 32$) all the valence electrons of the metal atom are transferred to the fullerene states, and the transferred charges are highly localized inside the fullerene and near the metal atom. The charge localization is a consequence of the strong metal-fullerene interaction. The counterintuitive picture established here corrects the widely accepted view of a metallofullerene as a "superatom" consisting of a metal cation surrounded by a fullerene anion. These findings allow evaluating more reliably the various physical properties of the fullerene-based nanomaterials.

ACKNOWLEDGMENTS

This work was supported by the U.S. DOE (Grant No. DEFG0205ER46209, and the Division of Materials Sciences and Engineering, Office of Basic Energy Sciences) and supplemented by the U.S. NSF (Grant No. DMR-0606485) and NSF of China. The calculations were performed at DOE NERSC and ORNL's Center for Computational Sciences.

[1] Y. Chai, T. Guo, C. Jin, R. E. Haufler, L. P. F. Chibante, J. Fure, L. Wang, J. M. Alford, and R. E. Smalley, J. Phys. Chem. **95**, 7564 (1991).

[2] H. Shinohara, Rep. Prog. Phys. **63**, 843 (2000).

[3] J. R. Heath, S. C. O'Brien, Q. Zhang, Y. Liu, R. F. Curl, H. W. Kroto, F. K. Tittle, and R. E. Smalley, J. Am. Chem. Soc. **107**, 7779 (1985).

[4] J. Lee, H. Kim, S.-J. Kahng, G. Kim, Y.-W. Son, J. Ihm, H. Kato, Z. W. Wang, T. Okazaki, H. Shinohara, and Y. Kuk, Nature (London) **415**, 1005 (2002); M. Mikawa, H. Kato, M. Okumura, M. Narazaki, Y. Kanazawa, N. Miwa, and H. Shinohara, Bioconjugate Chem. **12**, 510 (2001).

[5] S. Hino, H. Takahashi, K. Iwasaki, K. Matsumoto, T. Miyazaki, S. Hasegawa, K. Kikuchi, and Y. Achiba, Phys. Rev. Lett. **71**, 4261 (1993).

[6] L. Moro, R. S. Ruoff, C. H. Becker, D. C. Lorents, and R. Malhotra, J. Phys. Chem. **97**, 6801 (1993).

[7] E. Nishibori, M. Takata, M. Sakata, H. Tanaka, M. Hasegawa, and H. Shinohara, Chem. Phys. Lett. **330**, 497 (2000).

[8] K. Kobayashi and S. Nagase, Chem. Phys. Lett. **282**, 325

(1998).
[9] M. S. Dresselhaus, G. Dresselhaus, and P. C. Eklund, *Science of Fullerenes and Carbon Nanotubes* (Academic, San Diego, 1996), Chap. 8.
[10] X.-D. Wang, T. Hashizume, Q. Xue, H. Shinohara, Y. Saito, Y. Nishina, and T. Sakurai, Jpn. J. Appl. Phys., Part 2 **32**, L866 (1993).
[11] D. M. Poirier, M. Knupfer, J. H. Weaver, W. Andreoni, K. Laasonen, and M. Parrinello, Phys. Lett. B **49**, 17403 (1994).
[12] B. Kessler, A. Bringer, S. Cramm, C. Schlebusch, W. Eberhardt, S. Suzuki, Y. Achiba, F. Esch, M. Barnaba, and D. Cocco, Phys. Rev. Lett. **79**, 2289 (1997).
[13] J. Lu, X. Zhang, X. Zhao, S. Nagase, and K. Kobayashi, Chem. Phys. Lett. **332**, 219 (2000).
[14] L. Senapati, J. Schrier, and K. B. Whaley, Nano Lett. **4**, 2073 (2004).
[15] J. Lu, R. F. Sabirianov, W. N. Mei, Y. Gao, C. Duan, and X. C. Zeng, J. Phys. Chem. B **110**, 23637 (2006).
[16] G. Li, R. F. Sabirianov, J. Lu, X. C. Zeng, and W. N. Mei, J. Chem. Phys. **128**, 074304 (2008).
[17] D. Liu and F. Hagelberg, Int. J. Quantum Chem. **107**, 2253 (2007).
[18] S. Liu and S. Sun, J. Organomet. Chem. **599**, 74 (2000).
[19] D. S. Bethune, R. D. Johnson, J. R. Salem, M. S. de Vries, and C. S. Yannoni, Nature (London) **366**, 123 (1993).
[20] G. Kresse and J. Furthmüller, Phys. Rev. B **54**, 11169 (1996).
[21] D. M. Ceperley and B. J. Alder, Phys. Rev. Lett. **45**, 566 (1980).
[22] P. E. Blöchl, Phys. Rev. B **50**, 17953 (1994); G. Kresse and D. Joubert, *ibid.* **59**, 1758 (1999).
[23] H. J. Monkhorst and J. D. Pack, Phys. Rev. B **13**, 5188 (1976).
[24] J. P. Perdew and Y. Wang, Phys. Rev. B **45**, 13244 (1992).
[25] P. Ordejón, E. Artacho, and J. M. Soler, Phys. Rev. B **53**, R10441 (1996).
[26] N. Troullier and J. L. Martins, Phys. Rev. B **43**, 1993 (1991).
[27] E. Artacho, D. Sánchez-Portal, P. Ordejón, A. García, and J. M. Soler, Phys. Status Solidi B **215**, 809 (1999).
[28] R. S. Mulliken, J. Chem. Phys. **23**, 1833 (1955).
[29] R. Klingeler, P. S. Bechthold, M. Neeb, and W. J. Eberhardt, Chem. Phys. **113**, 1420 (2000).
[30] J. Lu, W. N. Mei, Y. Gao, X. Zeng, M. Jing, G. Li, R. Sabirianov, Z. Gao, L. You, J. Xu, D. Yu, and H. Ye, Chem. Phys. Lett. **425**, 82 (2006).
[31] G. W. Morley, B. J. Herbert, S. M. Lee, K. Porfyrakis, T. J. S. Dennis, D. Nguyen-Manh, R. Scipioni, J. van Tol, A. P. Horsfield, A. Ardavan, D. G. Pettifor, J. C. Green, and G. A. D. Briggs, Nanotechnology **16**, 2469 (2005).
[32] M. Chi, Z. Zhang, P. Han, X. Fang, W. Jia, H. Dong, and B. Xu, J. Mol. Model. **14**, 465 (2008).
[33] M. Takata, E. Nishibori, M. Sakata, C. R-Wang, and H. Shinohara, Chem. Phys. Lett. **372**, 512 (2003).
[34] W. Andreoni and A. Curioni, Appl. Phys. A: Mater. Sci. Process. **66**, 299 (1998).
[35] R. Tellgmann, N. Krawez, S.-H. Lin, I. V. Hertel, and E. E. B. Campbell, Nature (London) **382**, 407 (1996).